Organocatalytic-racemization reaction elucidation of aspartic acid by density functional theory

Natsuki Watanabe, Yuta Hori, Mitsuo Shoji, Mauro Boero, Yasuteru Shigeta

Organocatalytic-Racemization Reaction Elucidation of Aspartic Acid by Density Functional Theory

Abstract: Aldehydes and carboxylic acids are widely used as catalysts for efficient racemization process of amino acids. However, the detailed reaction mechanism remains unclear. This work aims to clarify the racemization mechanism of aspartic acid (Asp) catalyzed by salicylaldehyde and acetic acid by using computational approaches. Density functional theory was used to obtain the structures and relative energies of ten intermediates and five transition states, thus characterizing the main stages of the reaction. The calculated energy diagram shows that the dehydration step has the highest energy barrier, followed by the reaction step to change the chirality of Asp, which is a crucial process for racemization. In the dehydration reaction, water molecules can induce a remarkable decrease in the required energy.

Natsuki Watanabe,[a] Yuta Hori,*[b] Mitsuo Shoji,*[b,c] Mauro Boero,[d] and Yasuteru Shigeta[b]

Keywords: racemization, aspartic acid, organocatalytic reaction mechanism, density functional theory, Viedma ripening, salicylaldehyde, acetic acid

Introduction

Proteins in living organisms on Earth are composed of 20 different amino acids. All the natural amino acids, except glycine, have two enantiomeric forms (L and D) resulting from the asymmetric carbon center. Despite their identical physical and chemical properties, these enantiomers interact differently with chiral biomolecules. For instance, the typical taste receptors present in the human tongue are able to detect and recognize molecular chirality by specific interactions between the receptors and the chiral molecules. As a result, monosodium L- and D-glutamic acids exhibit umami and bitter properties, respectively. In general, a D/L-mixture of chiral molecule can be separated using optical resolution. The unwanted enantiomers which separated by this method can be recycled by changing them to a racemic mixture using a method called racemization. Therefore, racemization is an important step in the process of obtaining a single pure enantiomer. Racemization is often performed under harsh reaction conditions that include high temperatures and catalysis (acids, bases, or metal complexes).[1–3]

In previous studies[4,5], Yoshioka et al. developed a simple and versatile racemization reaction of α-amino acids, performed with neutral, acidic, and basic amino acids, catalyzed by organic molecules, aldehydes and carboxylic acids. Figure 1 shows a model reaction that proceeds through the initial formation of an intermolecular imine (C=N) bond between an amino acid and aldehyde, with the elimination of a water molecule. Subsequent protonation of the imine N atom by acetic acid forms an iminium cation. Subsequently, an acetate anion removes the α-proton of the iminium cation to form an achiral molecule. Because this reaction is reversible, the chiral inversion occurs when acetic acid delivers a proton to the opposite side of the original bond. The proton from the acetic acid is not donated regioselectively, so the racemization is complete when the system reaches equilibrium state after a sufficient amount of time. All reaction steps are reversible. Chirality can be exchanged via the achiral molecule by the forward and backward reaction processes.

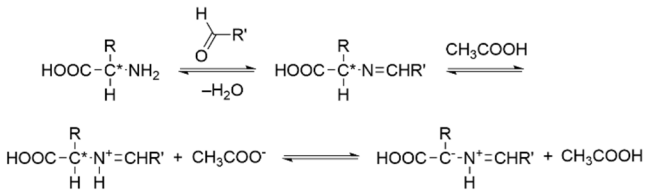

FIGURE 1. Proposed reaction scheme for the racemization of amino acids.[4] Asymmetric carbons are marked with an asterisk.

This organocatalytic reaction is an efficient and inexpensive method for amino acid racemization[6], and has been exploited upon incorporation into a solid-phase amino acid deracemization method termed Viedma ripening, showing to be competitive with respect to the available wide variety of other amino acid

[b] *Yuta Hori, Mitsuo Shoji, Yasuteru Shigeta*
Center for Computational Sciences
University of Tsukuba
1-1-1 Tennodai, Tsukuba, Ibaraki 305-8577, Japan
E-mail: hori@ccs.tsukuba.ac.jp, mshoji@ccs.tsukuba.ac.jp

[a] *Natsuki Watanabe*
Graduate School of Pure and Applied Sciences
University of Tsukuba
1-1-1 Tennodai, Tsukuba, Ibaraki 305-8571, Japan

[c] *Mitsuo Shoji*
JST-PRESTO
4-1-8 Honcho, Kawaguchi, Saitama 332-0012, Japan

[d] *Mauro Boero*
Institut de Physique et Chimie des Matériaux de Strasbourg,
University of Strasbourg
CNRS, UMR 7504, 23 rue du Loess, F-67034 France

Received: ((will be filled in by the editorial staff))
Revised: ((will be filled in by the editorial staff))
Published online: ((will be filled in by the editorial staff))

racemization methods (e.g. by using strong acids). Viedma ripening can be employed to obtain either L- or D-type enantiopure crystals.[7–12] Viedma provided the firs evidence for the deracemization phenomenon using sodium chlorate crystal.[7] His group also showed that pure enantiomeric crystals (conglomerates) of aspartic acid (Asp) can be obtained by growing the crystal during stirring and under racemization conditions.[8] Racemization by organocatalyst is an important process in Viedma ripening because of the enhancement of the process that this method is able to provide. In Viedma ripening of amino acids, salicylaldehyde and acetic acid are used for the racemization. Furthermore, this same method applied to other molecules such as sugars, 1,8-diazabicyclo[5.4.0]undec-7-ene is often used to catalyze the racemization.[13] Given this scenario, organocatalytic-racemization reactions are of fundamental interest in the Viedma ripening. Viedma ripening is an established mechanism for the enantiomeric amplification of chiral organic molecules. Furthermore, it is perceived as one of the reasons for the observed enantiomeric excess of amino acids in meteorites such as Murchison and Tagish Lake.[14–17] In this regard, understanding the mechanism of amino acid racemization can provide detailed information on various physical phenomena, including the Viedma ripening and the enantiomeric excesses in meteorites.

The detailed mechanism of this organocatalytic racemization reaction remains unclear. Thus, we analyzed the reaction pathway to unravel the role of the organocatalytic molecules and the relative energies of the various stages along the racemization reaction. Because the reaction takes place in an aqueous solution, zwitterionic amino acid species must be considered. Our theoretical insight into the structures and relative energies of intermediates and transition states in the racemization reaction of Asp is based on atomistic calculations using density functional theory (DFT). Our calculation results provide a basis for rationalizing the efficient amino acid racemization.

Methods

This study focused on the racemization reaction of Asp using salicylaldehyde and acetic acid via the reaction pathway shown in Figure 2. Asp has two types of carboxy groups, the pK_a values of which are 1.99 and 3.90, respectively. In this study, we consider the reactions in aqueous solution. For this reason, we assume a zwitterionic form of Asp with a bis-carboxylate structure. This reaction can be divided into three elementary steps: proton transfer from the amino group of Asp to salicylaldehyde and formation of an intermolecular C–N bond (Reaction 1), dehydration to form an iminium cation (Reaction 2), and acetate-catalyzed deprotonation to form an achiral molecule (Reaction 3).

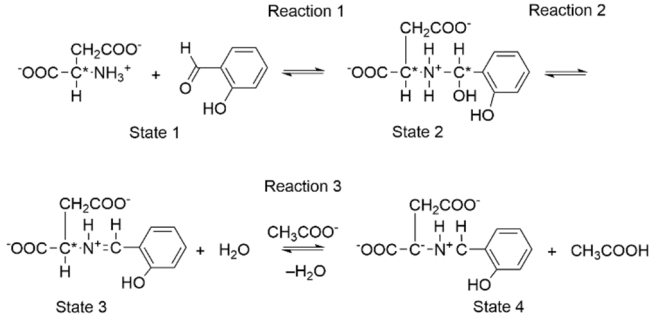

FIGURE 2. The reaction pathway for aspartic acid (Asp) racemization, catalyzed by salicylaldehyde and acetic acid used in our calculations. This reaction pathway consists of three elementary steps (Reactions 1–3). Asymmetric carbons are marked with an asterisk. The zwitterionic form of Asp was used as the reaction was performed in an aqueous medium.

Structural optimization, total energy calculation, and vibrational analysis were performed using DFT to search for intermediates and transition states. For each case, intrinsic reaction coordinates (IRCs) were calculated to confirm whether the reactants and products of each elementary reaction step were continuously connected via the realization of a corresponding transition state. Molecular exchange reactions were omitted from the IRC calculation. All DFT calculations were performed using the B3LYP functional with the 6-311++G(d, p) basis set, as implemented in the Gaussian 16 package.[18] The water solvation effect was accounted for using the polarizable continuum model.[19,20] We have assessed the reliability of the DFT method by reproducing the relative energies with an accuracy close to that of CCSD(T)/cc-pVTZ and absorption spectra.[21–24] Additionally, this DFT approach provides accurate atomic charge distribution and structures of protein-active sites.[25-27] We used Chemcraft software[28] to visualize the molecular structures.

Results and Discussion

Figure 3 shows the energy diagrams for the Asp racemization reaction, and the corresponding optimized structures are shown in Figure 4. The relative energies with respect to **IM1** were computed by a careful alignment of the stoichiometry of **IM1** with the other reaction states. More precisely, whenever some molecules were missing with respect to **IM1**, the energies of these missing molecules were added for compensation. Analogously, whenever extra molecules were present with respect to **IM1**, their energies were subtracted. Direct proton transfer from the amino group of Asp to the aldehyde group of salicylaldehyde is unlikely to occur because salicylaldehyde is a weak base (pK_a = −3), and the protonated intermediate is very unstable. Instead, we found a favorable three-step pathway involving proton transfer and acetic acid-assisted intermolecular bond formation between Asp and salicylaldehyde: **IM1**–**IM2**, **IM3**–**IM4**, and **IM5**–**IM6** (Figure 3(a)). Asp deprotonation occurs from **IM1** to **IM2** with a proton transfer to the acetate anion. At **IM1**, a proton of the amino group of Asp interacts with the acetate anion via a hydrogen bond, with N–H and O–H distances of 1.08 and 1.57 Å, respectively. As the reaction proceeds from **IM1** to **IM2**, the proton approached to the O atom of the acetate anion. At **TS1**, the N–H and the O–H distances become 1.39 and 1.14 Å, respectively, with a 2.42 kcal·mol^{-1} relative energy with respect to **IM1**. After the proton transfer, the O–H distance decreases to 1.08 Å at **IM2**, completing the deprotonation reaction. From **IM3** to **IM4**, the deprotonated Asp and salicylaldehyde molecules approached each other. The C–N distance decreases considerably from 4.73 Å **(IM3)** to 1.63 Å **(IM4)**, forming a covalent bond between the carbon atom of the salicylaldehyde and the N atom of Asp at **IM4**. The relative energy of **TS2** with respect to **IM1** is 18.3 kcal·mol^{-1}. In the pathway from **IM5** to **IM6**, the protonated acetic acid approaches the oxygen atom of the aldehyde group. **IM6** corresponds to State 2, shown in Figure 2. The O–H distance of the acetic acid increases from 1.05 Å in **IM5** to 1.39 Å in **IM6**, with an opposite decrease in the O–H distance of carbinolamine from 1.45 to 1.08 Å. The C–N distance between the carbon of salicylaldehyde and the amine group of Asp gradually decreases to 1.58, 1.56, and 1.55 Å during this reaction. The relative energy of **TS3** is 5.91 kcal·mol^{-1} with

respect to **IM1**. Contrary to the current belief that acetic acid only catalyzes the α-proton abstraction of the proton bound to the α-carbon in Figures 1 and 2, our calculations indicate that acetic acids can also catalyze the proton transfer in the salicylaldehyde-Asp complex (**IM1** to **IM2** and **IM5** to **IM6**).

The reaction from **IM7** to **IM8** in Figure 3(b) corresponds to Reaction 2 in Figure 2, in which one nitrogen-bonded hydrogen atom is transferred to the hydroxyl group of carbinolamine in a dehydration reaction. The O–H, C–O, and N–H distances in **IM7** are 2.24, 1.42, and 1.02 Å, respectively. In **TS4**, the O–H distance decreases to 1.14 Å, and the C–O and the N–H distances increase to 1.56 Å and 1.47 Å, respectively. One water molecule dissociates to form **IM8**. The relative energy of **TS4** with respect to **IM1** is 64.5 kcal·mol^{-1}. To complete the survey of this reaction, we also considered a proton shuttle process in which protons diffuse in water, confirming that the dehydration reaction is more viable reaction channel.

The reaction from **IM9** to **IM10,** shown in Figure 3(c), corresponds to Reaction 3, as shown in Figure 2. There, an acetate anion removes the α-proton from Asp to form an achiral imine intermediate; the C–H distance between the α-carbon and the proton was 1.09 Å at **IM9**, and the O–H distance of the acetate acid was 1.03 Å at **IM10**. The relative energy of **TS5** with respect to **IM1** is 35.2 kcal·mol^{-1}.

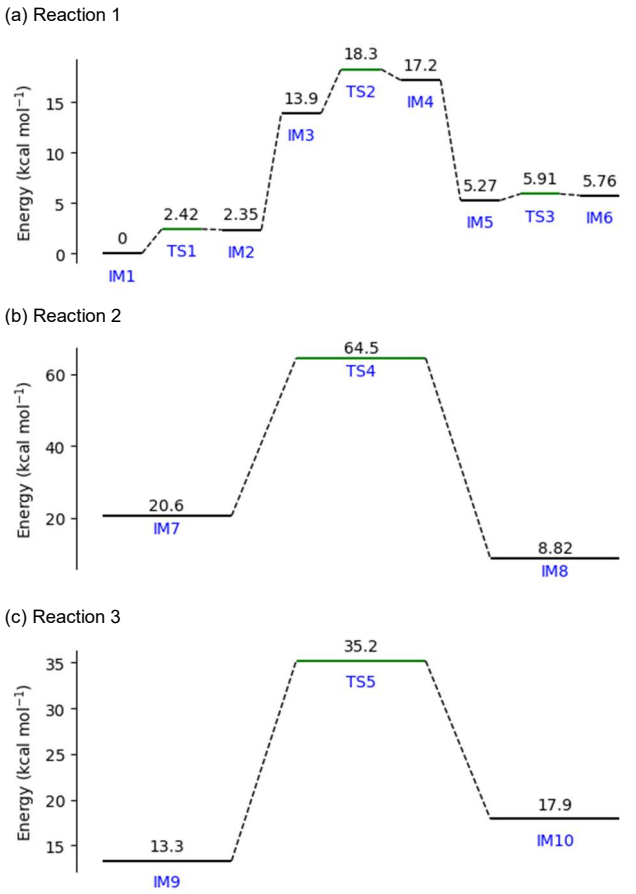

FIGURE 3. Calculated energy diagrams for the aspartic acid racemization reaction catalyzed by salicylaldehyde and acetic acid, including ten intermediates (**IM1**–**IM10**) and five transition states (**TS1**–**TS5**) corresponding to reaction 1 (a), reaction 2 (b), and reaction 3 (c) in Figure 2. The corresponding structures are shown in Figure 4.

While Reaction 1 (**IM1**–**IM6**) has a low-energy barrier, Reactions 2 and 3 have high-energy transition states of 64.5 kcal·mol^{-1} **(TS4)** and 35.2 kcal·mol^{-1} **(TS5)**, respectively. Reaction 3 is expected to occur because the Viedma's experiments are performed in aqueous reaction medium and high temperature of over 90 ºC.[8] Nevertheless, the calculated energy barrier of Reaction 2 is rather high and difficult to overcome, even at this temperature. Considering that this reaction takes place in aqueous solution, water molecules from the solvent can be explicitly taken into account for a better assessment of both the transition state structure and the associated energies. In fact, water molecules have previously been shown to catalyze a chiral inversion reaction of serine.[29] Our calculations show that the relative energy of **TS4** decreases with the increasing number of surrounding water molecules (Figure 5). **TS4**, **TS4-1**, and **TS4-2** contain zero, one, and two water molecules, respectively. In **TS4-1**, the initial conformation of a water molecule was arranged to form a hydrogen bond between the hydroxy group and the oxygen atom of the H_2O molecule. In **TS4-2**, another water molecule was added in the optimized **TS4-1** to form a hydrogen bond between this newly introduced H_2O molecule and the one interacting with the hydroxy group. Although a water molecule has two hydrogen bond donors to form a hydrogen bond with a neighbour H_2O molecule, we confirmed that the energy contribution due to the second water molecule (Figure 5(c) and Figure S2 in Supporting Information) was small in **TS4-2**. The relative energy decrease of 17.9 kcal·mol^{-1} to 46.6 kcal·mol^{-1} in **TS4-2** should allow the reaction to proceed because this energy is lower than that of the gas-phase Asp racemization (52.90 kcal·mol^{-1}, calculated at the DF-CCSD(T)/cc-pVTZ//M06-2X/aug-cc-pVTZ level).[30]

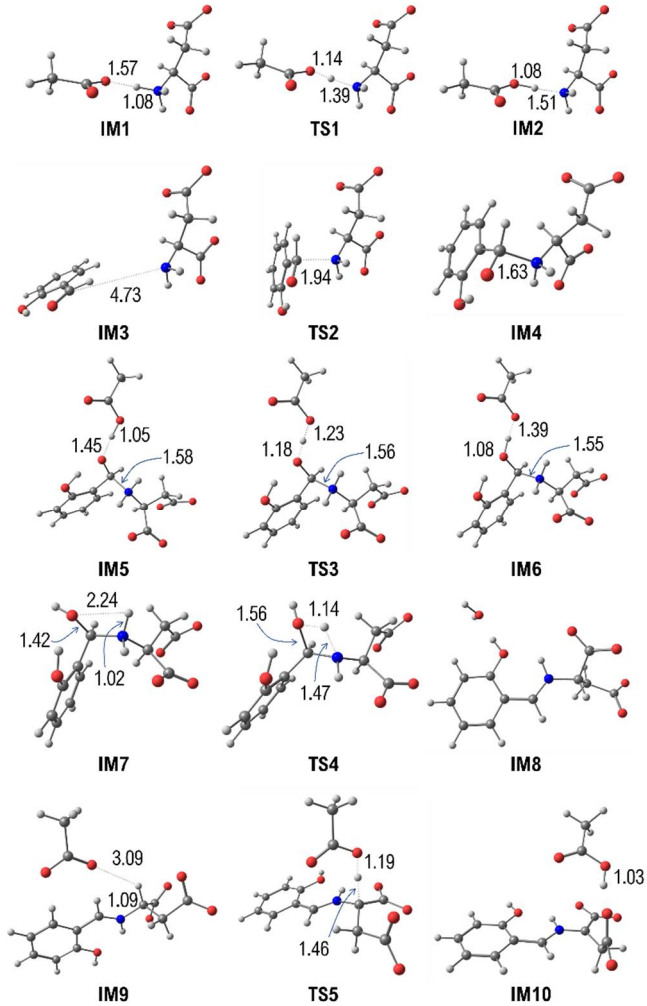

FIGURE 4. Optimized structures of intermediates and transition states shown in Figure 3. Lengths are given in Å. The labels correspond to those in Figure 3. The atoms were color coded as C-gray, O-red, N-blue, and H-white.

We investigated the influence of water molecules on the reaction by examining changes in the geometries and atomic charges of **IM7**, **TS4**, **TS4-1**, and **TS4-2**. By comparing the O–H, C–O, and N–H distances of **IM7** and **TS4**, we found that the O–H and N–H distances changed significantly. This indicates that proton migration from the N to O atoms is responsible for the energy barrier of this reaction step. The Mulliken atomic charges of oxygen in **TS4**, **TS4-1**, and **TS4-2** (Figure 5) are –0.135, –0.297, and –0.322, respectively, indicating that the negative charge increases with the number of water molecules. Therefore, the increased negative charge of the oxygen promotes proton migration, resulting in a lower energy barrier. This suggests that water acts as a catalyst in this reaction. If molecules capable of catalyzing this dehydration reaction are present, it is expected that leading to a more efficient racemization reaction of amino acids.

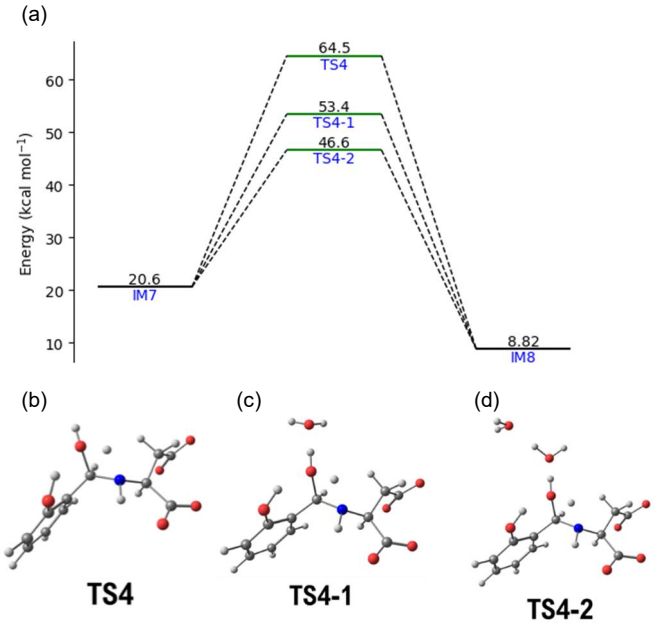

FIGURE 5. (a) Calculated energy diagram for the variable activation energies for **TS4** with the number of surrounding water molecules. The optimized structures **TS4 (b)**, **TS4-1 (c)**, and **TS4-2 (d)** have zero, one, and two water molecules, respectively.

Conclusion

In this study, we explored the mechanism of the racemization reaction of zwitterionic Asp catalyzed by salicylaldehyde and acetic acid using DFT. We identified ten intermediates and five transition states along the reaction path. Previous studies have suggested that acetic acid only catalyses the chirality-changing reaction (Reaction 3). We found that acetic acid also catalyzes other reaction steps, **IM1** to **IM2** and **IM5** to **IM6**. The transition state **TS4-2** had the highest relative energy, at 46.6 kcal·mol^{-1}, strongly influenced by the presence of water molecules. Therefore, the reaction can proceed at under the reported experimental conditions of over 90 °C. We conclude that efficient dehydration is crucial for this reaction step. The energy barrier of the chirality-changing reaction (35.2 kcal·mol^{-1} at **TS5**) is lower than that of the dehydration reaction. The amino acid reagent is regenerated in a racemic state via an inverse reaction (**IM10** to **IM1**), and the high-energy transition state **TS4** exists in both enantiomers. Therefore, our computational results provide new insights into the roles of salicylaldehyde, acetic acid, and water in the overall amino acid racemization reactions.

Acknowledgments

This work was partly supported by the JSPS Grants-in-Aid for Scientific Research (JP20H05453, JP20H05088, JP21H05419, and JP22H04916), MEXT Grants-in-Aid for Scientific Research on Innovative Areas (JP21H05419), JST PRESTO grant number JPMJPR19G6, and a research grant from The Mazda Foundation. Some computations were performed using computer facilities at the Research Institute for Information Technology, Kyushu University; the Research Center for Computational Science, Okazaki, Japan (Project:22-IMS-C122); and the Multidisciplinary Cooperative Research Program in CCS, University of Tsukuba. M.B. thanks the HPC Center at the University of Strasbourg funded by the Equipex Equip@Meso project, the CPER Alsacalcul/Big Data, and the Grand Equipement National de Calcul Intensif (GENCI) under allocation DARI-A0120906092 and A0140906092. We acknowledge Editage (www.editage.com) for English language editing.

Supporting information

Additional supporting information may be found in the online version of this article on the publisher's website.

REFERENCES AND NOTES

1. Schroeder RA, Bada JL. A review of the geochemical applications of the amino acid racemization reaction. *Earth-Sci. Rev.* **1976**;12:347–391.

2. Kawamura K, Yukioka M. Kinetics of the racemization of amino acids at 225–275 °C using a real-time monitoring method of hydrothermal reactions. *Thermochim. Acta* **2001**;375:9–16.

3. Smith GG, Khatib A, Reddy GS. The effect of nickel (II) and cobalt (III) and other metal ions on the racemization of free and bound L-alanine. *J. Am. Chem. Soc.* **1983**;105:293–295.

4. Yamada S, Hongo C, Yoshioka R, Chibata I. Method for the racemization of optically active amino acids. *J. Org. Chem.* **1983**;48:843–846.

5. Yoshioka R. Method for the racemization of optically active amino acids. *Top Curr. Chem.* **2007**;269:83–132.

6. Intaraboonrod K, Lerdwiriyanupap T, Hoquante M, Coquerel G, Flood AE. Temperature cycle induced deracemization. *Mendeleev Commun.* **2020**;30:395–405.

7. Viedma C. Chiral symmetry breaking during crystallization: complete chiral purity induced by nonlinear autocatalysis and recycling. *Phys. Rev. Lett.* 2005;94(6):065504.

8. Viedma C, Ortiz JE, Torres Td, Izumi T, Blackmond DG. Evolution of Solid Phase Homochirality for a Proteinogenic Amino Acid. *J. Am. Chem. Soc.* **2008**;130:15274–15275.

9. Spix L, Meekes H, Blaauw RH, van Enckevort WJP, Vlieg E. Complete Deracemization of Proteinogenic Glutamic Acid Using Viedma Ripening on a Metastable Conglomerate. *Cryst. Growth Des.* **2012**;12:5796–5799.

10. Li WW, Spix L, De Reus SC, Meekes H, Kramer HJ, Vlieg E, Ter Horst JH. Deracemization of a Racemic Compound via Its Conglomerate-Forming Salt Using Temperature Cycling. *Cryst. Growth Des.* **2016**;16:5563–5570.

11. Xiouras C, Van Cleemput E, Kumpen A, Ter Horst JH, Van Gerven T, Stefanidis GD. Towards Deracemization in the Absence of Grinding through Crystal Transformation, Ripening, and Racemization. *Cryst. Growth Des.* **2017**;17:882–890.

12. Putman JI, Armstrong DW. Recent advances in the field of chiral crystallization. *Chirality* **2022**;34:1338–1354.

13. Sanada K, Washio A, Ishikawa H, Yoshida Y, Mino T, Sakamoto M. Chiral Symmetry Breaking of Monoacylated Anhydroerythritols and *meso*-1,2-Diols through Crystallization-Induced Deracemization. *Angew. Chem. Int. Ed*. **2022**;61:e202201268; *Angew. Chem.* **2022**;134:e202201268.

14. Pizzarello S, Zolensky M, Turk KA. Nonracemic isovaline in the Murchison meteorite: chiral distribution and mineral association. *Geochim. Cosmochim. Acta* **2003**;67:1589–1595.

15. Glavin DP, Dworkin JP. Enrichment of the amino acid L-isovaline by aqueous alteration on CI and CM meteorite parent bodies. *Proc. Natl. Acad. Sci. USA* **2009**;106:5487–5492.

16. Friedrich JM, McLain HL, Dworkin JP, Glavin DP, Towbin WH, Hill M, Ebel DS. Effect of polychromatic X-ray microtomography imaging on the amino acid content of the Murchison CM chondrite. *Meteorit. Planet Sci.* **2019**;54:220–228.

17. Glavin DP, Elsila JE, McLain HL, Aponte JC, Parker ET, Dworkin JP, Hill DH, Connolly Jr HC, Lauretta DS. Extraterrestrial amino acids and L-enantiomeric excesses in the CM2 carbonaceous chondrites Aguas Zarcas and Murchison. *Meteorit. Planet. Sci.* **2021**;56:148–173.

18. Gaussian 16, Revision C.01, Frisch MJ, Trucks GW, Schlegel HB, Scuseria GE, Robb MA, Cheeseman JR, Scalmani G, Barone V, Petersson GA, Nakatsuji H, Li X, Caricato M, Marenich AV, Bloino J, Janesko BG, Gomperts R, Mennucci B, Hratchian HP, Ortiz JV, Izmaylov AF, Sonnenberg JL, Williams-Young D, Ding F, Lipparini F, Egidi F, Goings J, Peng B, Petrone A, Henderson T, Ranasinghe D, Zakrzewski VG, Gao J, Rega N, Zheng G, Liang W, Hada M, Ehara M, Toyota K, Fukuda R, Hasegawa J, Ishida M, Nakajima T, Honda Y, Kitao O, Nakai H, Vreven T, Throssell K, Montgomery Jr JA, Peralta JE, Ogliaro F, Bearpark MJ, Heyd JJ, Brothers EN, Kudin KN, Staroverov VN, Keith TA, Kobayashi R, Normand J, Raghavachari K, Rendell AP, Burant JC, Iyengar SS, Tomasi J, Cossi M, Millam JM, Klene M, Adamo C, Cammi R, Ochterski JW, Martin RL, Morokuma K, Farkas O, Foresman JB, Fox DJ. Gaussian, Inc., Wallingford CT, **2016**.

19. Tomasi J, Mennucci B, Cammi R. Quantum Mechanical Continuum Solvation Models. *Chem. Rev.* **2005**;105:2999–3093.

20. Cossi M, Barone V, Cammi R, Tomasi J. Ab initio Study of Solvated Molecules: A New Implementation of the Polarizable Continuum Model. *Chem. Phys. Lett.* **1996**;255:327–335.

21. Shoji M, Watanabe N, Hori Y, Furuya K, Umemura M, Boero M, Shigeta Y. Comprehensive search of stable isomers of alanine and alanine precursors in prebiotic syntheses. *Astrobiology* **2022**;22:1129–1142.

22. Watanabe N, Shoji M, Miyagawa K, Hori Y, Boero M, Umemura M, Shigeta Y. Amplification of Enantiomeric Excess of Amino Acids through dimerization in solution. **2023**, to be published.

23. Sato A, Shoji M, Watanabe N, Boero M, Shigeta Y, Umemura M. Origin of homochirality in amino acids induced by Lyα irradiation in the early stage of the Milky way. **2023**, to be published.

24. Shoji M, Kitazawa Y, Sato A, Watanabe N, Boero M, Shigeta Y, Umemura M. Enantiomeric excesses of aminonitrile precursors determine the homochirality of amino acids. *J. Phys. Chem. Lett.* **2023**. DOI://10.1021/acs.jpclett.2c03862

25. Shoji M, Murakawa T, Nakanishi S, Boero M, Shigeta Y, Hayashi H, Okajima T. Molecular mechanism of a large conformational change of the quinone cofactor in the semiquinone intermediate of bacterial copper amine oxidase. *Chem. Soc.* **2022**;13:10923–10938.

26. Mishima K, Shoji M, Umena Y, Shigeta Y, Biological advantage of the arrangements of C-phycocyanin chromophores in phycobilisome from the electronic energy transfer viewpoint. *Bull. Chem. Soc. Japan* **2023,** DOI:/10.1246/bcsj.20220334.

27. Hashimoto M, Miyagawa K, Singh M, Katayama K, Shoji M, Furutani Y, Shigeta Y, Kandori H. Specific Zinc Binding to Heliorhodopsin. *Phys. Chem. Chem. Phys.* **2023**;25:3535–3543.

28. Chemcraft – a graphical software for the visualization of quantum chemistry computations, https://www.chemcraftprog.com

29. Tong H, Liu YF, Yan H, Jiang C, Gao F, Mei Z, Hong K, Yang X, Wang Z., Theoretical investigation of the chiral transition of serine and the roles of water, hydroxyl radical and hydroxide ion. *New J. Chem.* **2019**;43(31):12340–12350.

30. Kaur R, Rani N, Vikas. Gas-phase stereoinversion in aspartic acid: reaction pathways, computational spectroscopic analysis, and its astrophysical relevance. *ACS Omega* **2018**;3:14431–14447.